ELSEVIER

Catalysis Today 70 (2001) 139–154

CATALYSIS TODAY

www.elsevier.com/locate/cattod

Infrared studies on SnO_2 and Pd/SnO_2

D. Amalric-Popescu, F. Bozon-Verduraz*

Laboratoire de Chimie des Matériaux, Divisés et Catalyse, Université Paris 7-Denis Diderot, 2 Place Jussieu, 75251 Paris Cedex 05, France

Abstract

The peculiarities of the IR studies of adsorption on semiconducting oxides are reviewed with special attention to SnO_2. Absorption by free electrons is very strong in reducing atmospheres and well-defined conditions are required to get vibrational information on the nature of surface species. CO adsorption on SnO_2 at room temperature (r.t.) gives rise to CO–Sn^{2+} and CO–Sn^{4+} end-on species and to various carbonate entities. NO adsorption leads to the formation of mononitrosyls, nitrite and nitrate species. Pd/SnO_2 catalysts are prepared according to original procedures: photodeposition and grafting of a molecular complex; the grafting method leads to highly dispersed PdO which is reduced to well-dispersed Pd upon CO adsorption at r.t., whereas NO gives rise to nitrosyl species mainly adsorbed on ionic Pd. The specificity of SnO_2 is evidenced upon interaction of a stoichiometric (CO + NO) mixture *at r.t.*: formation of N_2O on SnO_2 alone, generation of N_2O and isocyanate on PdO/SnO_2. These results are explained by the presence of oxygen vacancies and may be related to the low-temperature catalytic activity of SnO_2-supported palladium in deNO_x reactions reported elsewhere.

Keywords: FTIR spectroscopy; Tin dioxide; Palladium catalysts; CO adsorption; NO adsorption

1. Introduction

1.1. Peculiarities concerning the infrared studies of semiconducting oxides

The optical absorption of semiconducting oxides arises from five different phenomena [1]: (i) *intrinsic absorption*, corresponding to transitions between (full) valence bands and (empty) conduction bands, which occur often in the UV–visible range and sometimes in the near-infrared (NIR) (for narrow gap semiconductors); (ii) transitions between valence bands, called *intervalence transitions*, only observed in p-type materials, which may appear in the NIR; (iii) *free carrier absorption*, arising from transitions within one band; (iv) transitions of an electron to or from a localized state; (v) *lattice vibrational absorption*.

Semiconducting oxides are widely used in heterogeneous catalysis either as supports or active phases; when compared to *insulating oxides* such as silica, alumina or magnesia, their *mid-infrared* examination offers special difficulties due to mainly the transition types (iii) and (iv), which involve the absorbance due to free carriers and electron- or hole-donors, whose concentration depends on the semiconduction type, the surrounding atmosphere and the temperature.

In the case of n-type semiconductors (e.g. ZnO, TiO_2, CeO_2, SnO_2), a pretreatment in a *reducing* atmosphere generates *electron-donor levels* (oxygen vacancies V_O, metal under a lower oxidation state), which increases the free electron concentration; the semiconductor may even become *degenerate*, i.e. it may behave like a metal, showing a reflectivity edge and a plasma frequency. When the semiconductor is not degenerate, the absorption of conduction electrons is a function of $1/\nu^n$ with $2 < n < 3$ [1,2] and the increase of absorption is larger at low wavenumbers

* Corresponding author. Fax: +33-1-44-27-61-37.
E-mail address: bozonver@ccr.jussieu.fr (F. Bozon-Verduraz).

0920-5861/01/$ – see front matter
PII: S0920-5861(01)00414-X

(high wavelengths); this phenomenon may then preclude the observation of bulk and surface species as reported in the case of CeO_2 [3] and SnO_2 [4]. In addition to this background absorption, the presence of *electron-donor levels* gives rise to electronic transitions (type (iv)) which may occur in the infrared region:

$$M^{(n-1)+} \rightarrow M^{n+} + e^- \quad (1)$$

$$V_O \rightarrow V_O{}^+ + e^- \quad (2a)$$

$$V_O{}^+ \rightarrow V_O{}^{2+} + e^- \quad (2b)$$

Such transitions have been previously reported, e.g. Ce^{3+} in CeO_2 [3,5].

These difficulties are seriously enhanced when the sample under study is a metal supported on an n-type semiconducting support; the reduction of the support is then greatly favoured by the metal, e.g. through activation in vacuum and spill over of hydrogen or CO. It follows that the absorbance may decrease to zero, especially when the reducing gas is adsorbed at temperature higher than the ambient. For example, this has been observed in the case of metals supported on ZnO [6] and ceria [7].

For a given support, the reducibility depends on the texture, the morphology and the conditions of pretreatment. Heating the sample in oxygen at a convenient temperature allows one to maintain the transmittance at an acceptable level as oxygen can act as an *electron trap*. For example, adsorption of oxygen on a non-stoichiometric oxide, containing *oxygen vacancies* V_O, generates lattice oxygen $O_O{}^x$ (removing the donor levels):

$$\tfrac{1}{2}O_{2(g)} + V_O \rightarrow O_O{}^x \quad (3)$$

according to the Kröger–Vink notation [2].

It follows that the electron concentration in the solid decreases and that the sample transmittance increases.

Hence the study of adsorbed species in reducing atmosphere requires the conditions of examination to be carefully chosen.

1.2. The case of tin dioxide

Tin dioxide is an n-type semiconductor. Its band gap width E_g amounts to 3.6 eV [8,9]. It is transparent in the visible range in its undoped form, which has been applied to the production of transparent conductive coatings [10]. When heated in reducing atmosphere (vacuum, hydrogen, carbon monoxide), it becomes non-stoichiometric by losing oxygen, which generates tin cations with unsaturated coordination (4 instead of 6) [11]; it is believed that the point defects are oxygen vacancies and Sn^{2+} ions [2,11], whose thermal excitation may give rise to paramagnetic species such as $V_O{}^+$ (F-centre) and Sn^{3+} [12,13]. As its electrical conductivity is very sensitive to oxidative and reducing atmospheres, SnO_2 is widely used in sensors [8,14] and a large amount of publications and patents have appeared. Moreover, the adsorption of a series of molecules has been studied, especially by Harrison et al. [15–19,59,60] for 30 years.

Conversely, tin dioxide has received limited attention in the catalysis field and the use of Sn–Sb oxides in selective oxidation appears to be a unique industrial application [20]. Moreover, the ability of SnO_2 to generate defects has been only recently shown to induce interesting performances for supported Pd catalysts, e.g. in deNO_x reactions [21]. The present paper concerns first the infrared study of high surface area SnO_2 at various temperatures and under different surrounding atmospheres; the surface and bulk species present in vacuum or in oxygen (OH, Sn–O–Sn, etc.) are examined as well as the interactions with CO_2, CO, NO and (CO + NO). The second part concerns the examination of Pd/SnO_2 catalysts; it focuses on the influence of the pretreatment on the nature of the species formed upon adsorption of CO and NO.

A prerequisite for sensing and catalytic applications is the preparation of high surface area tin dioxide; the procedure used is described below.

2. Experimental

2.1. Samples preparation

High surface area tin dioxide (174 m^2/g) was prepared through reaction of metallic tin with concentrated nitric acid, centrifugation of the suspension obtained, washing of the solid with distilled water and drying at 120°C [22].

SnO_2-supported Pd samples were obtained according to the following procedures, original on SnO_2 and already presented elsewhere [21]: (i) *oxidized sample (GC)*: *grafting* of Pd acetylacetonate on tin dioxide

from a solution in toluene at 110°C for 4 h, filtering, drying of the grafted support at 80°C for 12 h and *calcination* under flowing oxygen at 400°C for 2 h; (ii) *reduced sample (PH)*: *photodeposition* of Pd on the support by irradiation of a suspension of SnO_2 in a $Pd(NO_3)_2$ solution (pH = 2.0–2.8); the source was a mercury lamp and 2-propanol was used as hole scavenger; after filtration, the solid was dried at 80°C for 12 h. The Pd content, determined by emission spectroscopy (ICP), was 3.0% for both samples; the mean Pd particle size was about 1.8–2 nm (from TEM) for the GC sample and 4.4 nm (from XRD broadening) for the PH sample.

2.2. Methods

FTIR transmission spectra were recorded on a Perkin-Elmer 1730 and on a Bruker Equinoxe spectrometers (resolution 4 cm^{-1}, 50 scans); the samples were pressed into self-supporting discs (about 25 mg/cm^2) and placed in a stainless steel cell (In Situ Research Instruments) allowing in situ analysis of samples in the 20–500°C range, including CO adsorption.

3. IR studies on SnO_2

Several bands due to fundamentals, overtones and combinations of OH, Sn–O and Sn–O–Sn entities appear in the 4000–800 cm^{-1} range; below 800 cm^{-1} there occurs the cut-off arising from lattice vibrations. In order to explore with a suitable resolution in the region 400–1000 cm^{-1}, the spectrum of a sample calcined at 500°C in air (surface area: 62 m^2/g) was recorded after dispersion in a KBr matrix (Fig. 1).

The results and the proposed attributions are presented in Table 1 and compared with the data published in the literatures [15,23–35]. The discrepancies concerning these attributions are due to several factors: (i) the nature of the sample (monocrystal, powder, colloidal suspension) and the proportion of low-coordination sites [36]; (ii) the stoichiometry of the oxide, i.e. the presence of intrinsic defects; (iii) the presence of impurities, i.e. extrinsic defects; (iv) the size and shape of the particles [61,62]; (v) the hydroxyl groups concentration.

A detailed account of all these factors appears to overcome the frame of this paper; additional work is certainly needed in particular to check the intervention of *electronic transitions* in the infrared range, proposed by Ghiotti et al. [4,29–32].

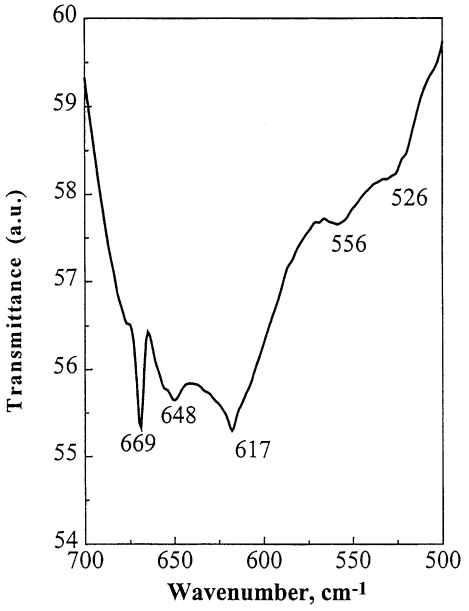

Fig. 1. IR spectrum of SnO_2 calcined at 500°C (KBr) in the 700–500 cm^{-1} range.

3.1. FTIR spectra after outgassing at various temperatures

The spectra were recorded at room temperature (r.t.) after outgassing (10^{-5} Torr) the as-prepared SnO_2 sample at various temperatures (100–500°C) for 15 h (Fig. 2). After evacuation at 100°C, the spectrum shows several bands: a peak at 3500 cm^{-1}, a broad band centred around 3000 cm^{-1} [ν_{OH}(Sn–OH)], two peaks at 2440 cm^{-1} [$2\delta_{OH}$(Sn–OH)] and 1610 cm^{-1} [$\delta_{OH}(H_2O)$] and bands at 1250, 1180, 960 and 874 cm^{-1} assigned to δ_{OH}(Sn–OH) (Table 1). Outgassing at 200°C removes the band located near 1610 cm^{-1} and the shoulder around 874 cm^{-1}, decreases the intensity of the bands at *2442*, 1251, 1180 and 960 cm^{-1}, whereas new bands appear at 1524 and 1420 cm^{-1}. Evacuation at 300°C shifts the hydroxyl band to 3190 cm^{-1} and removes the bands at *2442* and 960 cm^{-1}.

Until 300°C, the transmission increases with the outgassing temperature, especially at low wave-

Table 1
IR band positions and assignments for SnO_2

ν (cm^{-1})	Reference	Fundamental vibrations[a]	Overtones and combinations
300 [23,24]; 312 [25]	[23–25]	ν(Sn–O)	
526*; 540 [26]; 556*; 561 [27]	[26,27], this work*	ν(Sn–O, T)	
610 [25]	[25]	ν(Sn–O)	
(617, 648)*	This work*	ν(Sn–O)	
650 [23]	[23]	ν(Sn–O)	
(665, 667) [26]; 680 [27]; 669*	[26,27], this work*	ν(O–Sn–O)	
670 [25]; 690 [23]	[23,25]	ν(Sn–O)	
(737; 770) [16]	[15]	ν_{as}(Sn–O–Sn)	
870 [16]	[15]	ν_{as}(Sn–OH)	
934 [27]	[27]	δ_{OH}(Sn–OH, T)	
950 [16]	[15]	δ_{OH}(Sn–OH, T)	
(960, 1000, 1060, 1120) [23]	[23]		Lattice
1175 [16]; (1177–1180)*; 1242 [27]; 1245 [16]; (1245–1250)*	[15,27], this work*	δ_{OH}(Sn–OH, T)	
(1370, 1520) [23]	[23]		Lattice
(1378–1382)*	This work*		Lattice
1436 [16]; (1420–1436)*	[15], this work*		$2\nu_{as}$(Sn–O–Sn)
1536 [16]; (1520–1536)*	[15], this work*		$2\nu_{as}$(Sn–O–Sn)
(1610–1623)*; 1636 [28]; 1640 [16]	[15,28], this work*	$\delta_{OH}(H_2O)$	
(2429–2442)*	This work*		$2\delta_{OH}$(Sn–OH, T)
2900 [33]; 3000 [27]	[27,33]	ν_{OH}(Sn–OH, B)	
(3000–3500)* [33]	[33], this work*	ν_{OH}(Sn–OH, B)	
(2900–3400) [27]	[27]	ν(OH···O, B)	
3160 [29,30]; 3400 [33–35]	[29–35]	ν_{OH}(Sn–OH, B)	
3640 [16,29–32]; 3655*; (3740, 3830) [33]	[15,29–33], this work*	ν_{OH}(Sn–OH, T)	

[a] T: terminal; B: bridged.

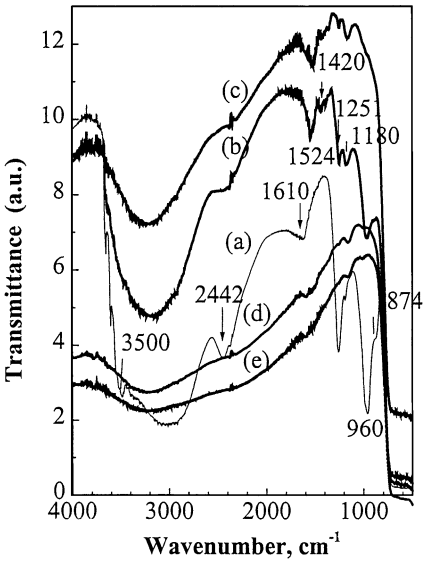

Fig. 2. IR spectra of SnO_2 outgassed at: (a) 100°C; (b) 200°C; (c) 300°C; (d) 400°C; (e) 500°C.

numbers. This phenomenon may be explained by the dependence of the light intensity diffused by the sample (Id) on the particle size (d) and on the frequency ν, which is expressed by $Id \approx d^3\nu^4$ [37]. As a consequence, Id decreases with ν and the sample transmittance increases when ν diminishes. After outgassing at 400°C, a drastic loss of transmission is observed. Only a weak shoulder near 1180 cm^{-1} is detected (spectrum d). This fall of transmission is assigned to the presence of free electrons created upon outgassing (that is in reducing conditions); the electron-donor levels have been evidenced by UV–visible spectra [21] and EPR measurements [38,63]. Even after outgassing at 500°C a broad hydroxyl band centred around 3200 cm^{-1} and a very small shoulder near 1180 cm^{-1} are still present, which may be explained by the presence of strongly bound hydroxyl groups encapsulated in the oxide bulk [39].

In order to differentiate the vibrations due to OH groups from those due to the Sn–O–Sn bridges, a

sample outgassed at 200°C during 4 h, was treated with D_2O vapour at r.t. ($p = 18$ Torr) during 15 min, and then evacuated at 200°C. Hydrogen–deuterium exchange was rapid. The broad band centred around 3190 cm^{-1} generates two bands: one located at 2639 cm^{-1}, the other at 2511 cm^{-1}; the bands at 1250 and 1180 cm^{-1} disappear and they probably move towards frequencies lower than 1000 cm^{-1}. The bands at 1524 and 1420 cm^{-1} were not modified by the D_2O treatment; they should be ascribed to vibration harmonics of Sn–O–Sn bridges obtained by condensation of hydroxyl groups. Outgassing at high temperature should increase the concentration of these species; however, such treatment leads also to a marked decrease of transmission, decreasing the sensitivity of detection of all entities; hence a pretreatment procedure minimizing the transmission losses was carried out.

3.2. Influence of a pretreatment in oxygen

To avoid the loss of transmission due to the partial reduction of the oxide, the SnO_2 sample dried at 120°C was pretreated first at 400°C in oxygen (1 h) and then cooled in vacuum from 400°C to r.t.; the surface area was then equal to 90 m^2/g.

Fig. 3 shows the influence of this pretreatment on the spectrum of SnO_2. The initial spectrum (a), recorded after outgassing at r.t., presents several bands which were ascribed above. After the pretreatment (spectrum b), the transmission is significantly higher and only residual hydroxyl groups, characterized by a broad band around 3000 cm^{-1} (ν_{OH}) and a weak shoulder at around 960 cm^{-1} (δ_{OH}), are still present; the bands at 1524 and 1420 cm^{-1} (see Fig. 2) are not observed; this means that the oxygen pretreatment has markedly decreased the concentration of Sn–O–Sn bridges.

Once more the transmission increases below 2500 cm^{-1} because the losses arising from diffused light decrease. The resulting sample may be considered as free from carbonates species and presents an appreciable transmittance. This pretreatment will then be employed as a standard procedure.

3.3. CO_2 adsorption

Various carbonate and related species may form upon CO_2 or CO adsorption on the surface of metal oxides and detailed assignment is not straightforward [40,41]; in contrast with other oxides of catalytic interest, a few IR studies have concerned the interaction of CO_2 with tin dioxide [15]; in the present work, CO_2 was only used as a probe to characterize the tin dioxide sample submitted to the standard procedure. The experiments were performed under 50 Torr at r.t.; several bands (Fig. 4) appear at about 1724, 1586, 1541 (shoulder), 1432, 1375, 1300, 1272 (shoulder), 1227 and 1050 cm^{-1}; after outgassing at r.t., the band at 1724 cm^{-1} disappears, the other bands decrease in intensity and the shoulder near 1540 cm^{-1} is better resolved. This complex spectrum may involve weakly adsorbed CO_2, unidentate and bidentate carbonate together with bicarbonate species; Table 2 (upper part) presents the assignments proposed with a reference to previous works.

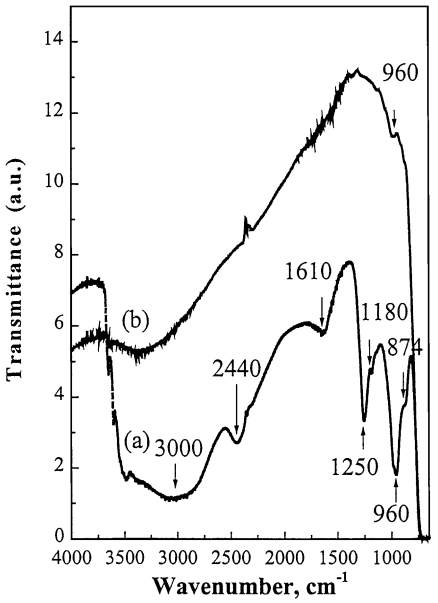

Fig. 3. Spectra of SnO_2: (a) outgassing at r.t.; (b) after calcination and outgassing at 400°C.

3.4. CO adsorption

Upon contact with CO, the sample suffers a significant transmission decrease, indicative of an increase of the electron concentration that is a partial reduction of the sample, described below by Eqs. (7)–(8b). Hence the experiments were performed at low CO

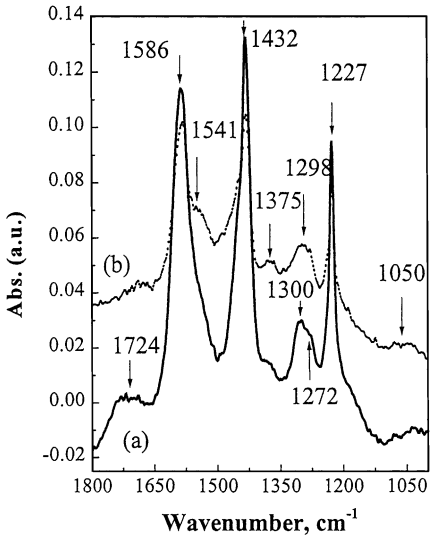

Fig. 4. IR spectrum of CO_2 adsorbed on SnO_2: (a) under CO_2 (50 Torr); (b) after outgassing at r.t.

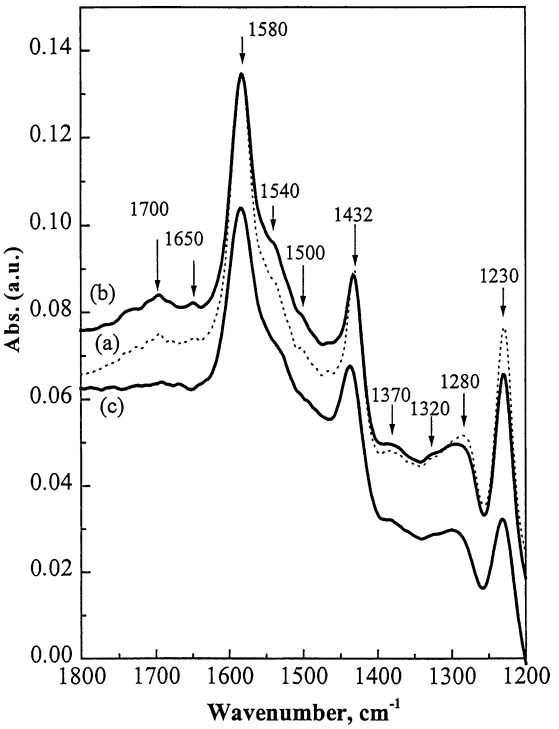

Fig. 5. IR spectra (1800–1200 cm^{-1}) of CO adsorbed on SnO_2: (a) under 6 Torr; (b) under 30 Torr; (c) after outgassing at r.t.

pressure ($\leq$30 Torr); carbon monoxide was introduced at r.t. (10 min) and the gaseous phase was evacuated at the same temperature. The spectra were recorded at r.t. and presented after subtracting the spectra of the gas phase and of the solid before adsorption. (i) *In the 1800–1200 cm^{-1} region* (Fig. 5), the band positions in the spectrum of the adsorbed phase are similar to those obtained upon CO_2 adsorption but their relative intensities are different, indicating a different distribution of the adsorbed species and possibly the presence of carboxylates (Table 2, lower part) [4,15–19].

Upon outgassing at r.t., the band at 1700 cm^{-1} is almost removed but the intensity of the other bands is only slightly decreased. The formation of carbonate species through contact with CO implies the existence of reactive oxygen on SnO_2 after the pretreatment at

Table 2
Band positions and assignments for CO_2 and CO adsorption on SnO_2 (1800–1000 cm^{-1})

Adsorbate	Reference	Carboxylate	Unidentate	Bidentate	Adsorbed CO_2	Bicarbonate
CO_2	This work (Fig. 4)		1432–1375	1586, 1280–1300, 1050	1724	1541, 1432, 1227
	[15]		1440–1450, 1370–1380			1596, 1300, 1225
CO	This work (Fig. 5)	1500–1320	1500, 1370	1580, 1280	1700	1540, 1432, 1230
	[4]		1480–1473, 1380–1370	1550–1538, 1320–1310, 1030–1022		1590–1585, 1443–1438, 1228–1225
	[15]		1440, 1370			
	[19]	1540, 1300	1500–1422, 1401–1320	1590–1600, 1223–1275	1700, 1180 (organic carbonate)	1585, 1295, 1225

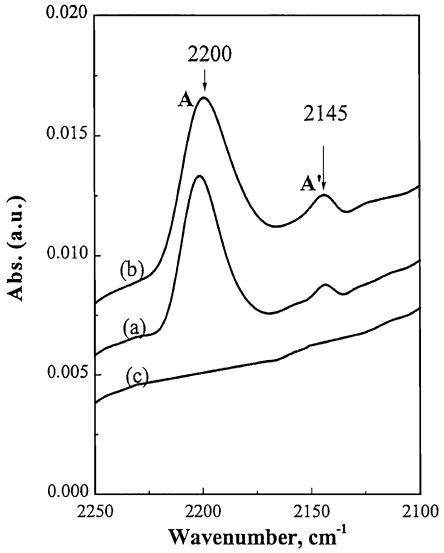

Fig. 6. IR spectra (2250–2100 cm^{-1}) of CO adsorbed on SnO_2: (a) under 6 Torr; (b) under 30 Torr; (c) after outgassing at r.t.

400°C. (ii) *In the 2500–2000 cm^{-1} range* (Fig. 6): bands attributed to "on-top" CO–Sn^{4+} (2200 cm^{-1}) and CO–Sn^{2+} entities (2145 cm^{-1}) [21].

The drastic loss of background transmission induced by CO adsorption is partially suppressed upon outgassing at r.t. (not shown); this means that the electron concentration is decreased, that is, the reduction by CO is partially reversible.

The creation of donor levels Sn^{2+} and oxygen vacancies as well as the variations of background transmission may be described as follows:

1. *upon outgassing pretreatments*: point defects are formed as shown by UV–visible diffuse reflectance spectroscopy [38,63]:

$$SnO_2 \rightleftharpoons SnO_{2-x} + \tfrac{1}{2}xO_{2(g)} \quad (4)$$

$$O_O{}^x \rightleftharpoons V_O + \tfrac{1}{2}O_{2(g)} \quad (5)$$

$$Sn^{4+} + V_O \rightleftharpoons Sn^{2+} + V_O{}^{2+} \quad (6)$$

2. *upon CO adsorption*:

$$CO_{(ads)} + O_O{}^x \rightleftharpoons CO_{2(g)} + V_O \quad (7)$$

The increase in electron concentration arises from

$$V_O \rightleftharpoons V_O{}^+ + e^- \quad (8a)$$

$$V_O{}^+ \rightleftharpoons V_O{}^{2+} + e^- \quad (8b)$$

$$Sn^{2+} \rightleftharpoons Sn^{4+} + 2e^- \quad (9)$$

where V_O, $V_O{}^+$ and $V_O{}^{2+}$ are the neutral and ionized oxygen vacancies, respectively, $O_O{}^x$ is the lattice oxygen, according to the Kröger–Vink notation [2].

3.5. NO adsorption

The adsorption of N_xO_y compounds on metals and metal oxides gives rise to a variety of species and has been very recently reviewed by Hadjiivanov [42]. Among the great number of papers, a few were devoted to SnO_2 [29] or SnO_2 containing transition metal ions of the first series [30,59,60].

In the present work, NO adsorption was carried out at different temperatures on a SnO_2 sample pretreated at 400°C as above.

3.5.1. Influence of NO pressure at room temperature

Several bands ascribed to nitrite and nitrate species [43–46] appear between 1700 and 1000 cm^{-1}, whereas nitrosyl entities are observed in the 1800–2000 cm^{-1} range (Fig. 7): (i) under 0.15 Torr (spectrum a) appear only very weak peaks at 1565, 1548, 1280, 1175 and 1010 cm^{-1}; (ii) when the NO pressure increases to 0.3 Torr (spectrum b), the bands cited above are markedly intensified whereas additional bands or shoulders are detected at 1617, 1450, 1220, and 1115 cm^{-1}; (iii) under 2 Torr (spectrum c), a further increase of intensity is noted together with the appearance of new bands at 1900 and 1850 cm^{-1} and of shoulders at around 1507 and 1045 cm^{-1}.

After evacuation at r.t. (spectrum d), the peaks at 1900 and 1850 cm^{-1} disappear, indicating that the nitrosyl species are weakly adsorbed on Sn^{4+}; conversely no change is noticed in the 1700–1000 cm^{-1} region, showing that the nitrite and nitrate entities are more firmly held. Table 3 (upper part) presents the assignments proposed; it is relevant to note that: (i) the band attribution of nitrite and nitrate is only tentative; (ii) the formation of N_2O was previously observed on SnO_2 at r.t. together with nitrites but without nitrates [29], and also reported upon interaction of NO with TiO_2 anatase [47]; the absence of N_2O in the present work may arise from the pretreatment in

Table 3
Band positions (cm^{-1}) and assignments for NO adsorption on SnO_2, oxidized Pd/SnO_2 and some related systems

System	Reference	N_2O adsorption on the support	Linear nitrosyls (DN: dinitrosyls)			Bridged nitrosyls, Pd^0	Nitrites on the support, unidentate (U), chelating (C)	Nitrates on the support, bidentates (BD), bridging unidentates (BU)
			Sn^{4+}	Pd^{2+}, Pd^+	Pd^0			
SnO_2	This work (Figs. 7 and 8)		1900, 1850				1450, 1370 (U); 1510, 1175 (C)	1545–1580, 1280, 1045 (BD); 1627, 1220, 1010 (BU)
	[29]	2236	1826				1280, 1175 (C)	
Pd/SnO_2	This work (Figs. 14 and 15)			1820–1825, 1788–1800	1730, 1753	1685–1690		1582–1586, 1280, 1045 (BD)
Pd/Al_2O_3	[49]	2232				1632–1599 (μ_2); 1580–1572 (μ_3)		
	[50]	2240		1815, 1855	1715	1612, 1463, 1240 (including adsorbed NO_2)		
Pd/SiO_2	[51]				1740, 1600 (bent)	1690, 1570		
Pd/zeolite	[52]			1840–1850	1878, 1908, 1839 (DN)			

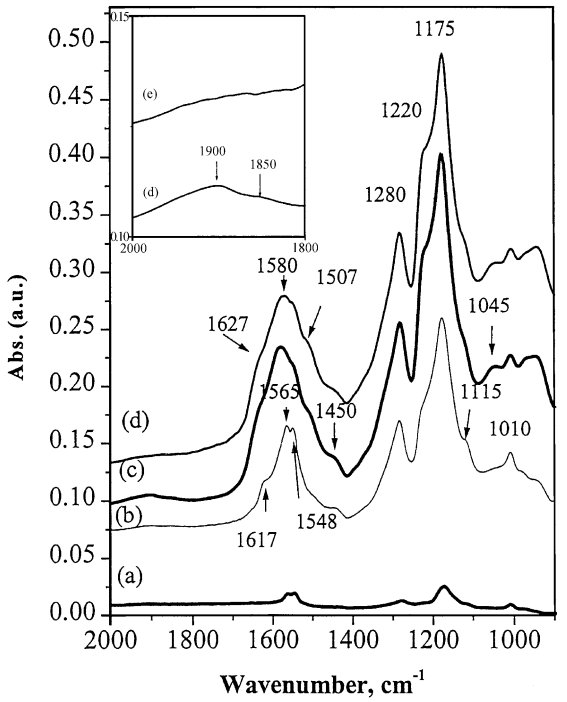

Fig. 7. IR spectrum of NO adsorbed on SnO_2: influence of NO pressure: (a) under 0.15 Torr; (b) under 0.3 Torr; (c) under 2 Torr; (d) after outgassing at r.t.

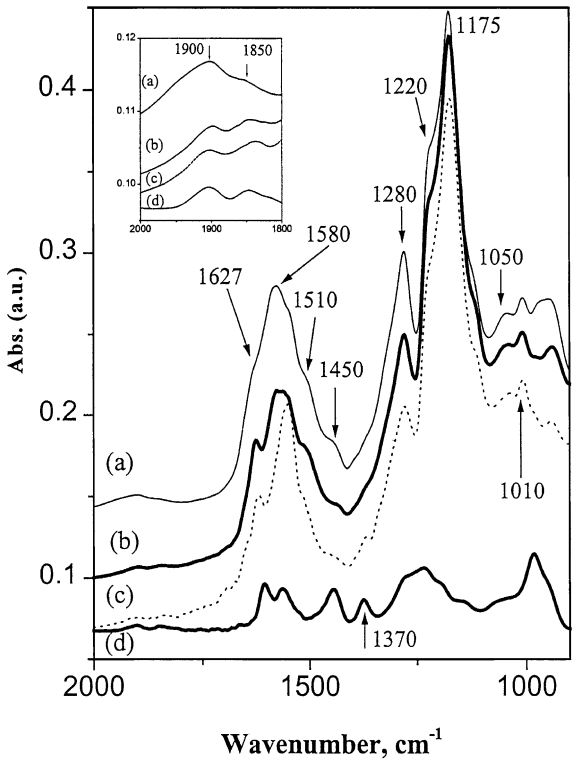

Fig. 8. IR spectra of NO adsorbed on SnO_2 under 2 Torr at different temperatures: (a) r.t.; (b) 50°C; (c) 100°C; (d) 200°C.

oxygen which decreases the concentration of oxygen vacancies, which are believed to induce the formation of nitrous oxide (see Eq. (11)).

3.5.2. *Influence of the adsorption temperature*

The spectra obtained under 2 Torr in the 25–200°C range are presented in Fig. 8. After adsorption at 50 and 100°C (spectra b and c) better resolved peaks appear between 1650 and 1500 cm^{-1}; after outgassing at 100°C (not shown), the intensity of all bands does not change significantly.

If the adsorption is carried out at 200°C (spectrum d) the intensity of all peaks is decreased, even though the pressure is increased up to 4 Torr; however, after evacuation at 200°C (not shown), they are still present including those ascribed to the nitrosyl species.

3.6. (CO + NO) *adsorption*

Adsorption at r.t. (Fig. 9) of a stoichiometric mixture (3 Torr CO, 3 Torr NO) led to the appearance of: (i) two peaks at 2238 cm^{-1} (N_2O) [29,30] and 2200 cm^{-1} (Sn^{4+}–CO) [21]; (ii) a series of bands at 1700, 1580, 1545, 1430, 1280, 1230, 1170 and 1040 cm^{-1}, assigned as above to various carbonate (Table 2), nitrite and nitrate species (Table 3). The comparison with Fig. 8 shows that in the presence of CO the nitrosyls are transformed into N_2O. It may involve the reaction:

$$CO + 2NO \rightarrow N_2O + CO_2 \quad (10)$$

since the bands assigned to CO_2 (1700 cm^{-1}) and bicarbonates are enhanced (1580, 1430 and 1230 cm^{-1}); but N_2O may also arise from the reaction of NO with oxygen vacancies induced by CO adsorption on the support (Eq. (7)):

$$2NO + V_O \rightarrow N_2O + O_O{}^x \quad (11)$$

Upon outgassing at r.t., the peaks located at 2238 and 2200 cm^{-1} disappear and the intensity of the other bands decreases markedly. The weak stability of the

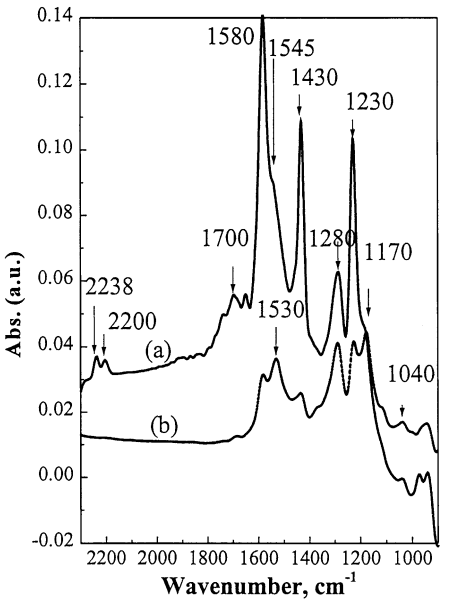

Fig. 9. IR spectra recorded upon interaction of a (CO + NO) stoichiometric mixture with SnO_2 at r.t.: (a) under 6 Torr; (b) after outgassing at r.t.

peaks at *2238* and 2200 cm^{-1} confirms their respective attribution to N_2O and Sn^{4+}–CO rather than to isocyanate species [18,42].

4. Pd/SnO_2 samples

Two types of catalysts were used (cf. Section 2):

1. In *oxidized* form (GC): calcination of the grafted sample at 400°C during 4 h followed by cooling under vacuum down to r.t.
2. In *reduced* form (PH): after *photodeposition*, drying at 120°C and evacuation at r.t.

4.1. CO adsorption

CO adsorption was carried out at r.t. or at a fixed temperature Tads. Upon contact with 100 Torr CO, the sample suffers a strong transmission decrease, ascribed to an increase of electron concentration (reduction of the carrier); in order to limit this phenomenon, the procedure was the following: introduction of CO under 3 Torr, then increase up to 30 Torr, evacuation first at r.t. during 15 min, then at 100°C during 1 h. The spectra were recorded "in situ" at the adsorption temperature.

4.1.1. CO adsorption on the oxidized sample (GC)

4.1.1.1. CO adsorption at room temperature. The 1800–1200 cm^{-1} region (not shown) contains a series of bands assigned to carbonates (mono and bidentate) and to bicarbonates already present on SnO_2 (cf. Table 2); the intensities are somewhat different, which indicates a different distribution of these species.

In the 2300–1800 cm^{-1} interval (Fig. 10 and Table 4), four bands appear:

- at 2200 cm^{-1} (A) ascribed to Sn^{4+}–CO,
- at 2144 cm^{-1} (B) assigned to Pd^{2+}–CO [53–55],
- at 2098 cm^{-1} (D) ascribed to Pd^{0}–CO [44,55,56],
- at 1930 cm^{-1} (E) with a shoulder (F) around 1895 cm^{-1} assigned to bridged species [44,55,56].

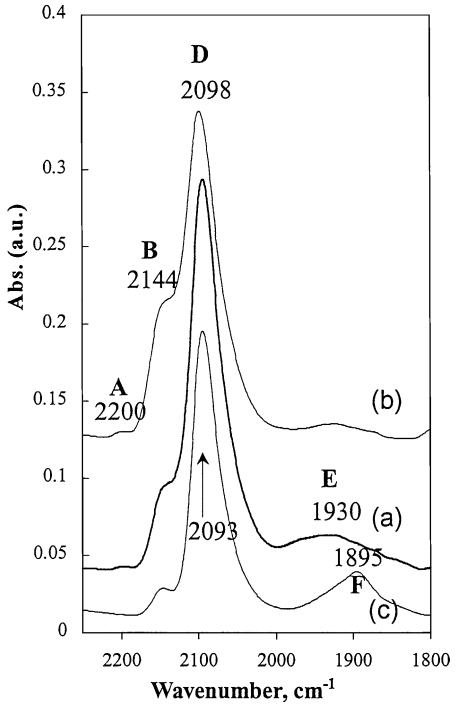

Fig. 10. Oxidized catalyst (GC): IR spectra (2300–1800 cm^{-1}) of CO adsorbed at r.t.: (a) under 5 Torr; (b) under 15 Torr; (c) after outgassing at r.t.

Table 4
IR bands (2300–1800 cm^{-1}) of CO adsorbed on SnO_2 and Pd/SnO_2 with reference to Pd/alumina

ν (cm^{-1})	Species	Reference
2200	$O{\equiv}C–Sn^{4+}$	This work
2145	$O{\equiv}C–Sn^{2+}$	This work
2160–2145	$O{\equiv}C–Pd^{2+}$	This work, Pd/alumina [44,53–56]
2135–2110	$O{\equiv}C–Pd^{+}$	This work, Pd/alumina [44,53–56]
2100–2025	$O{\equiv}C–Pd^{0}$	This work, Pd/alumina [44,53,55,56]
1995–1960	$Pd_2(CO)$ compressed or bridged on (1 0 0) faces	This work, Pd/alumina [53,55,56]
1950–1925	$Pd_2(CO)$ isolated or bridged on (1 1 1) faces	This work Pd/alumina [53,55,56]
1900–1800	$Pd_3(CO)$	This work Pd/alumina [53,55,56]

UV–visible diffuse reflectance experiments (not shown), were also performed to discriminate the influence of the pretreatment on the electronic state of Pd from that of CO adsorption. After the pretreatment in oxygen, the spectrum presents a broad band centred at about 465 nm ascribed to Pd^{2+} ions or PdO clusters [7,48]; upon outgassing at 400°C, this band is slightly weakened; after contact with 100 Torr CO at r.t., it is markedly decreased within less than 30 min and the sample colour turns from yellow to grey. This means that the sample is slightly reduced in vacuum and suffers a strong reduction upon contact with CO.

Hence the Pd^0 entities detected above (bands D and F) arise mainly from the reduction of Pd^{2+} species by CO, leaving only residual ionic Pd species (b and B) (Table 4). After outgassing at r.t. (Fig. 10, spectrum c), A disappears and B suffers a marked decrease, which confirms the attribution (these species are less firmly bonded because no retrodonation occurs); in addition, a weak displacement of band D towards lower wavenumbers is observed owing to the decrease of the dipole space coupling of the CO vibrators [55,56]. The high linear/bridged intensity ratio and the absence of compressed bridged species show that the metal is highly dispersed on the carrier.

4.1.1.2. CO adsorption at 50 and 100°C. After adsorption at 50°C (Fig. 11), the band B is almost undetectable, the D peak located initially (at r.t.) at 2095 cm^{-1} moves to 2087 cm^{-1} and is weakened, whereas the F peak is reinforced. This tendency may be explained by the achievement of the reduction of palladium and the sintering of the Pd particles, the increase of the metal particle size leading to a decrease of the linear/bridged intensity ratio (L/B + L). This

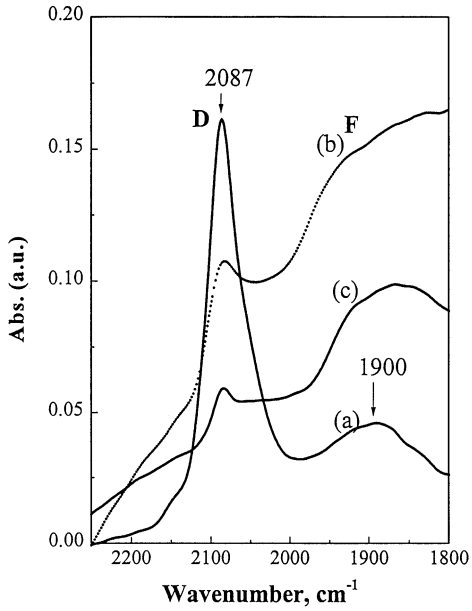

Fig. 11. Oxidized catalyst (GC): IR spectra (2300–1800 cm^{-1}) of CO adsorbed at 50°C: (a) under 5 Torr; (b) under 15 Torr; (c) after outgassing at r.t.

phenomenon becomes more marked when the pressure increases (not shown) and when the adsorption temperature reaches 100°C (Fig. 12). At this temperature, under 15 Torr CO, there is also an increase of the background absorbance arising from the reduction of SnO_2 (increase of electron concentration).

4.1.2. CO adsorption on the reduced sample (PH)

After CO adsorption at r.t., the spectrum of the solid obtained by photoreduction (PH) (Fig. 13) presents a weak band (B) at 2163 cm^{-1}, a shoulder (C) at 2125 cm^{-1}, an intense peak (D) at 2080 cm^{-1} and a

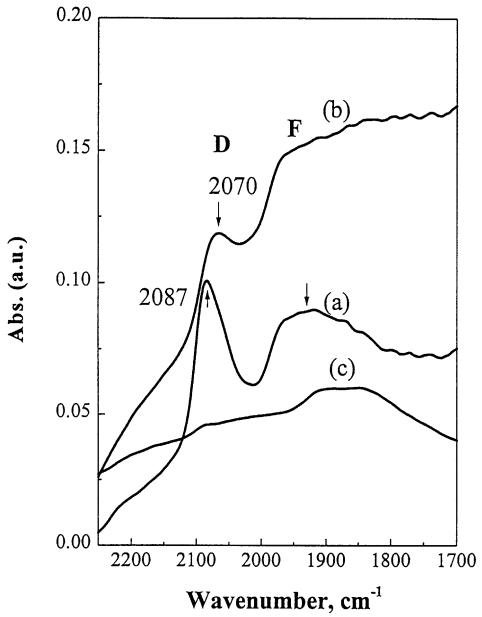

Fig. 12. Oxidized catalyst (GC): IR spectra (2300–1800 cm^{-1}) of CO adsorbed at 100°C: (a) under 0.1 Torr; (b) under 7 Torr; (c) after outgassing at r.t.

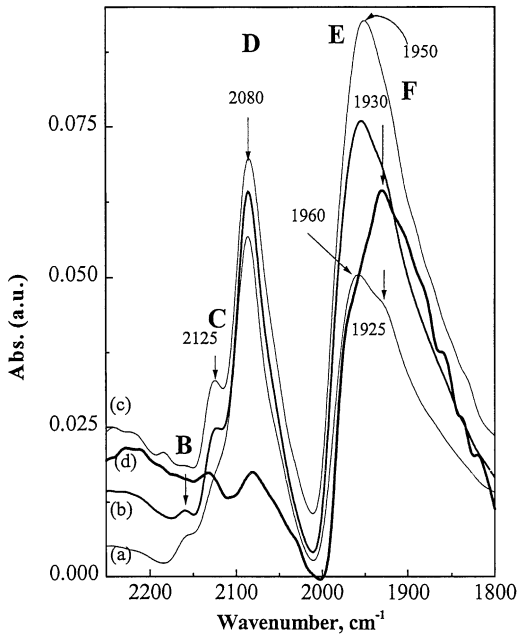

Fig. 13. Reduced catalyst (PH): IR spectra of CO adsorbed at r.t.; influence of CO pressure: (a) 5 Torr; (b) 15 Torr; (c) 35 Torr; (d) after outgassing at r.t.

strong broad band (E) centred around 1960 cm^{-1} with a shoulder F around 1925 cm^{-1}.

The intensity of C–F increases with the CO pressure in the 5–35 Torr range; decreasing the pressure to 10 Torr has no noticeable effect (not shown); after outgassing at r.t. (spectrum d) only small peaks at 2127 and 2080 cm^{-1} and an intense band at 1930 cm^{-1} (with a shoulder near 1950 cm^{-1}) are still present; finally, after outgassing at 150°C during 1 h (not shown), these bands disappear almost completely.

The attributions have been given above (Table 4). The main observations are: (i) the presence of *residual* Pd^{+} and Pd^{2+} species, which shows that the photoreduction is not complete, in agreement with the results obtained by photoelectron spectroscopy (XPS) [38,63]; (ii) the predominance of the bridged species compared to the linear species; this indicates that the dispersion is lower than in the case of the oxidized sample (GC).

4.2. NO adsorption

The experiments have been conducted only on the oxidized sample. The results obtained and the assignments are collected in Table 3, with reference to Pd/alumina [49,50], Pd/silica [51] and Pd/zeolite [52].

4.2.1. Influence of NO pressure at room temperature

Adsorption at r.t. (Fig. 14, spectra a–c) led to a series of bands and shoulders at 1788, 1730 1690, and 1550 cm^{-1}. Increasing NO pressure intensifies all bands and induces the appearance of a shoulder near 1825 cm^{-1}. Outgassing at r.t. (spectrum d) brings no significant changes; upon outgassing at 200°C (spectrum e), the bands in the 1825–1650 cm^{-1} range are markedly decreased, whereas a shoulder at 1612 cm^{-1} (bidentate nitrate) becomes detectable. The peaks at 1825 and 1788 cm^{-1} are ascribed to linear nitrosyl species on Pd^{2+} and Pd^{+}, respectively; the peaks at 1730 and 1685–1690 cm^{-1} are assigned to linear and twofold (μ_2) bridged species on Pd^{0}, respectively [49–52]. Note that the peak at 1685–1690 cm^{-1} is especially resistant to outgassing, which supports the assignment to bridged species on Pd.

4.2.2. Influence of the adsorption temperature

Fig. 15 compares the spectra recorded under 2 Torr at different temperatures. Increasing the adsorption

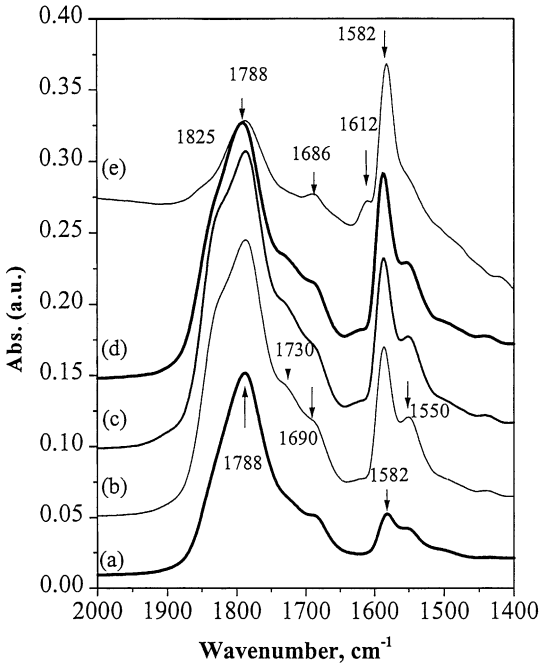

Fig. 14. Oxidized catalyst (GC): IR spectra of NO adsorbed at r.t.; influence of NO pressure: (a) under 0.15 Torr; (b) under 0.9 Torr; (c) under 2 Torr; (d) after outgassing at r.t.; (e) after outgassing at 200°C.

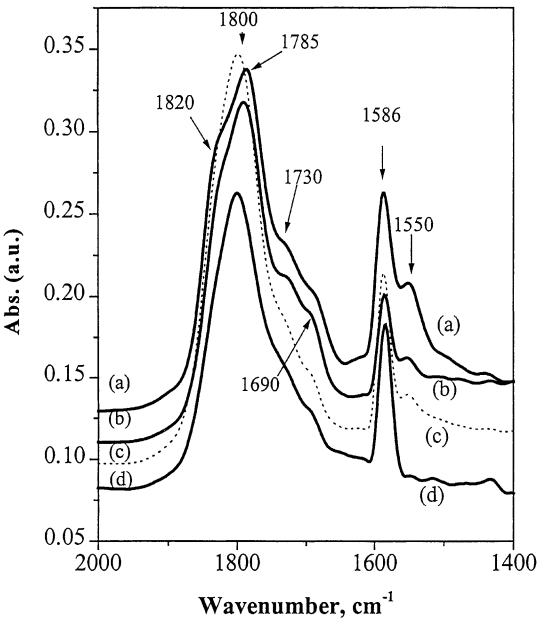

Fig. 15. Oxidized catalyst (GC): infrared spectra of NO adsorbed under 2 Torr at different temperatures: (a) r.t.; (b) 50°C; (c) 100°C; (d) 200°C.

temperature to 50°C (spectrum b) does not bring significant changes but, at 100°C (spectrum c), there is an upward shift of the main peak (1785–1800 cm^{-1}), suggesting an increase of the proportion of (NO)–Pd^{2+} species. Upon adsorption at 200°C (spectrum d), the same features are observed but the peak at 1550 cm^{-1} becomes very weak. After outgassing at 200°C (not shown) the intensity of the peak at 1585 cm^{-1} is not affected, which shows that the species involved is firmly bonded. Conversely, the band at 1800 cm^{-1} is markedly weakened. After outgassing at 300°C all bands are almost removed.

As a conclusion, when the adsorption temperature increases, the concentration of nitrates decreases, whereas the concentration of nitrosyl species adsorbed on Pd^0 and Pd^{2+} does not change. This may explain

Table 5
Band positions (cm^{-1}) and assignments of nitrosyl, carbonyl and related species for (CO + NO) adsorption on oxidized Pd/SnO_2 with reference to Pd/alumina

	Reference	Isocyanate	N_2O	Linear (L) and bridged (B) nitrosyls			Linear (L) and bridged (B) carbonyls	
				Sn^{4+}	Pd^{2+}, Pd^{+}	Pd^0	Pd^{+}	Pd^0
Pd/SnO_2	This work (Fig. 16)	2165 (Pd–NCO)	2235[a]	2211[b] (L)	1790 (L); 1825 (B)	1745 (L); 1700 (B)	2135 (L)	2095
Pd/Al_2O_3	[57]	2254 (Pd–NCO)				1750–1780	2133 (L)	2065 (L); 1936 (B)
	[58]	2241 (Al–NCO)			1779, 1796	1754, 1652 (bent)		2083 (L); 1966 (B)

[a] Observed at 2238 cm^{-1} on SnO_2.
[b] Observed at 2200 cm^{-1} on SnO_2.

that the deNO$_x$ activity of Pd/SnO$_2$ approaches 100% at 200°C [21].

4.3. CO + NO *adsorption*

The experiments have been conducted only on the oxidized sample (GC). The assignments are summarized in Table 5, taking into account the data obtained on the support alone (Section 3.6 and Tables 2 and 3). After adsorption of a stoichiometric CO + NO mixture at r.t. (Fig. 16), several peaks are observed in the spectral region 2300–1400 cm^{-1}: (i) two bands at 2235 and 2211 cm^{-1} ascribed to N_2O and to end-on CO adsorbed on Sn^{4+}, respectively; (ii) three peaks at 2165, 2135 and 2095 cm^{-1} whose assignment is discussed below; (iii) a strong band at 1790 cm^{-1} ascribed to bridged NO adsorbed on Pd^{n+} with a shoulder at 1745 cm^{-1} assigned to linear NO species on Pd^0; (iv) a shoulder at 1700 cm^{-1} assigned to bridged NO adsorbed on Pd^0; (v) a series of bands in the 1650–1000 cm^{-1} range, assigned to nitrite, nitrate and carbonate species (Tables 2 and 3). After evacuation at r.t. (Fig. 16, spectrum b), the peaks at 2235 and 2211 cm^{-1} and the shoulders at 1745 and 1650 cm^{-1} disappear, whereas the peak at 2165 cm^{-1} is accentuated. In addition, new bands or shoulders become visible at 1825 cm^{-1} (linear NO adsorbed on Pd^{2+}) and 1620 cm^{-1} (nitrates).

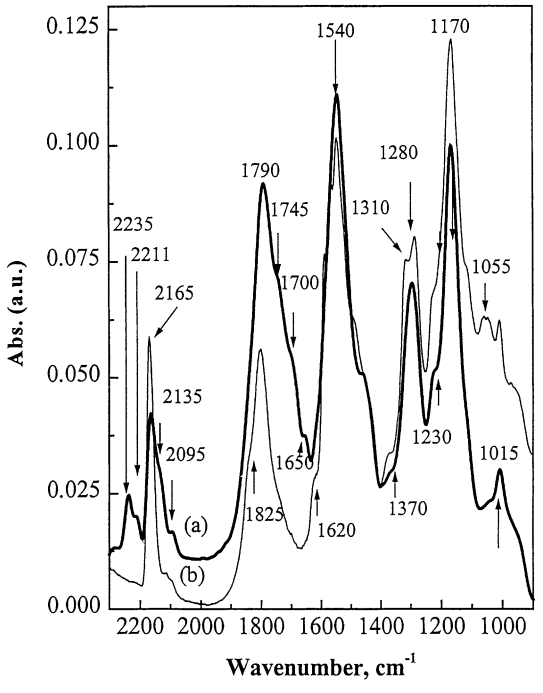

Fig. 16. Oxidized catalyst (GC): infrared spectra recorded upon interaction with a stoichiometric (CO + NO) mixture at r.t.: (a) under 6 Torr; (b) after outgassing at r.t.

The persistence of the band at 2165 cm^{-1} in vacuum suggests that it should be assigned to an isocyanate Pd–NCO rather than to a Pd^{2+}–CO species. Moreover, the band at 2095 cm^{-1} is much less intense than in the presence of CO alone (Fig. 10).

It may be concluded that adsorption of a stoichiometric (CO + NO) mixture: (i) delays the reduction of Pd^{2+} to Pd^0 by CO, and (ii) generates weakly adsorbed N_2O and more strongly held nitrosyl and isocyanate species.

5. Conclusions

The IR transmission of SnO_2, n-type semiconductor, is sharply decreased by electron absorption and the quality of vibrational information concerning the surface species depends strongly on the nature of the pretreatment. Outgassing at 400°C creates low-coordination Sn^{4+} and Sn^{2+} cations able to adsorb CO end-on species vibrating around 2200 and 2145 cm^{-1}, respectively. CO adsorption also generates various carbonate species, which implies the existence of reactive oxygen. NO adsorption at r.t. leads to the formation of mononitrosyl species weakly adsorbed on Sn^{4+} cations together with strongly held nitrites and nitrate species; when the adsorption temperature increases, the contribution of the latter decreases.

For the preparation of Pd/SnO$_2$ catalysts, the grafting of a molecular complex on SnO_2 leads to a larger dispersion than the photodeposition method: it generates highly dispersed PdO, which is reduced to well-dispersed Pd^0 upon CO chemisorption at r.t., giving rise mainly to end-on CO, a few bridged species and some residual Pd^{2+}(CO) entities, whereas NO gives rise to linear and bridged nitrosyls mainly adsorbed on ionic Pd; these entities are also observed upon adsorption of a (CO + NO) mixture together with N_2O and isocyanate species. The presence of NO delays the reduction of Pd^{2+} to Pd^0 by CO.

The specificity of SnO_2 is evidenced upon interaction of a stoichiometric (CO + NO) mixture *at r.t.*:

formation of N_2O on SnO_2, generation of N_2O and isocyanate on PdO/SnO_2, whereas, on alumina and Pd/alumina, temperatures higher than 200°C are required [57,58,64]. This peculiarity may be related to the presence of oxygen vacancies which has been evidenced elsewhere by UV–visible diffuse reflectance spectroscopy and electrical conductivity measurements [38,63]. These oxygen vacancies are believed to account for the low-temperature catalytic activity of SnO_2-supported palladium in deNO_x reactions [21].

References

[1] J.T. Houghton, S.D. Smith, Infrared Physics, Oxford University Press, Oxford, 1966, p. 117.
[2] P.A. Cox, Transition Metal Oxides, Clarendon Press, Oxford, 1995.
[3] F. Bozon-Verduraz, A. Bensalem, J. Chem. Soc., Faraday Trans. 90 (1994) 653.
[4] G. Ghiotti, A. Chiorino, F. Boccuzzi, Sensors and Actuators B 19 (1989) 151.
[5] C. Binet, A. Badri, M. Boutonnet-Kizling, J. Lavalley, J. Chem. Soc., Faraday Trans. 90 (1994) 1023.
[6] G. Ghiotti, F. Bocuzzi, A. Chiorino, Mater. Chem. Phys. 29 (1991) 65.
[7] A. Bensalem, J.C. Muller, D. Tessier, F. Bozon-Verduraz, J. Chem. Soc., Faraday Trans. 92 (1996) 3233.
[8] G. Heiland, Sensors and Actuators 2 (1982) 343.
[9] D.F. Cox, T.B. Fryberger, S. Semancik, Surf. Sci. 224 (1989) 121.
[10] M.K. Carpenter, D.A. Corrigan, Proceedings of the Symposium on Electrochromic Materials, Vol. 90, No. 2, 1989, p. 201.
[11] V.A. Gercher, D.F. Cox, J.M. Themlin, Surf. Sci. 306 (1994) 279.
[12] M.I. Ivanovskaya, G.A. Branitskii, D.R. Orlik, S.I. Malchenko, A.I. Vrublevskii, Russ. J. Inorg. Chem. 37 (5) (1992) 577.
[13] C. Canevali, N. Chiodini, P. Nola, F. Morazzoni, R. Scotti, C. Bianchi, J. Mater. Chem. 7 (6) (1997) 997.
[14] J.F. Aller, T. Moseley, J.O. Norris, D.E. Williams, J. Chem. Soc., Faraday Trans. I 83 (1987) 1323.
[15] E.W. Thornton, P.G. Harrison, J. Chem. Soc., Faraday Trans. 71 (1975) 461.
[16] P.G. Harrison, E.W. Thornton, J. Chem. Soc., Faraday Trans. 72 (1976) 2604.
[17] P.G. Harrison, E.W. Thornton, J. Chem. Soc., Faraday Trans. I 74 (1978) 2597.
[18] P.G. Harrison, A. Guest, J. Chem. Soc., Faraday Trans. 83 (1987) 3383.
[19] P.G. Harrison, A. Guest, J. Chem. Soc., Faraday Trans. 85 (1989) 1897.
[20] G. Centi, F. Trifiro, Catal. Rev. 28 (1986) 165.
[21] D. Amalric-Popescu, F. Bozon-Verduraz, Catal. Lett. 64 (2000) 125.
[22] J. Donaldson, M.J. Fuller, J. Inorg. Nucl. Chem. 30 (1968) 1083.
[23] R. Summitt, N.F. Borrelli, J. Phys. Chem. Solids 26 (1965) 921.
[24] R. Summitt, J.A. Marley, N.F. Borrelli, J. Phys. Chem. Solids 25 (1964) 1465.
[25] J.R. Ferraro, Low-frequency Vibrations of Inorganic and Coordination Compounds, Vol. 74, Plenum Press, New York, 1970.
[26] J.C. Giuntini, W. Granier, J.V. Zanchetta, A. Taha, J. Non-Cryst. Solids 9 (1990) 1383.
[27] B. Orel, U. Lavrencic-Stangar, Z. Crnjak-Orel, P. Bukovec, M. Kosec, J. Non-Cryst. Solids 167 (1994) 272.
[28] A. Bertoluzza, C. Fagnano, M.A. Morelli, V. Gottardi, M. Guglielmi, J. Non-Cryst. Solids 48 (1982) 117.
[29] A. Chiorino, F. Boccuzzi, G. Ghiotti, Sensors and Actuators B 5 (1991) 189.
[30] G. Ghiotti, A. Chiorino, W.X. Pan, L. Marchese, Sensors and Actuators B 7 (1992) 691.
[31] G. Ghiotti, A. Chiorino, W.X. Pan, Sensors and Actuators B 15–16 (1993) 367.
[32] G. Ghiotti, A. Chiorino, G. Martinelli, M.C. Carotta, Sensors and Actuators B 24–25 (1995) 520.
[33] R.S. Hiratsuka, C.V. Santilli, D.V. Silva, S.H. Pulcinelli, J. Non-Cryst. Solids 147–148 (1992) 67.
[34] R.T. Presecatan, S.H. Pulcinelli, C.V. Santilli, J. Non-Cryst. Solids 147–148 (1992) 340.
[35] F. Bréhat, B. Wyncke, J.M. Léonard, Y. Dussausoy, Phys. Chem. Minerals 17 (1990) 191.
[36] P. Hollins, Surf. Sci. Rep. 16 (1992) 51.
[37] M.L. Hair, Infrared Spectroscopy in Surface Chemistry, Marcel Dekker, New York, 1967, p. 59.
[38] D. Amalric-Popescu, J.M. Herrmann, F. Bozon-Verduraz, Proceedings of the 12th International Congress on Catalysis, Stud. Surf. Sci. Catal. B 130 (2000) 1307.
[39] G. Pfaff, J.P. Bonnet, M. Onillon, P. Hagenmuller, Eur. J. Solid State Inorg. Chem. 27 (1990) 367.
[40] G. Busca, V. Lorenzelli, Mater. Chem. 7 (1982) 89.
[41] J.C. Lavalley, Catal. Today 27 (1996) 377.
[42] K.I. Hadjiivanov, Catal. Rev.-Sci. Eng. 42 (2000) 71.
[43] G. Socrates, Infrared Characteristic Group Frequencies, Tables and Charts, Wiley, New York, 1989, pp. 149, 208, 217, 238, 242.
[44] A.A. Davydov, in: C.H. Rochester (Ed.), Infrared Spectroscopy of Adsorbed Species on the Surface of Transition Metal Oxides, Wiley, New York, 1990.
[45] J. Laane, J.R. Ohlsen, Prog. Inorg. Chem. 27 (1980) 466.
[46] K. Nakamoto, Infrared and Spectra of Inorganic and Coordination Compounds, 5th Edition, Part B, Wiley, New York, 1997.
[47] G. Ramis, G. Busca, V. Lorenzelli, P. Forzatti, Appl. Catal. 64 (1990) 243.
[48] A. Rakaï, D. Tessier, F. Bozon-Verduraz, New J. Chem. 16 (1992) 869.
[49] T.E. Hoost, K. Otto, K.A. Laframboise, J. Catal. 155 (1995) 303.

[50] M. Valden, R.L. Keiski, N. Xiang, J. Perc, J. Aaltonen, M. Pessa, T. Maunula, A. Savimäki, A. Lahti, M. Hrkönen, J. Catal. 161 (1996) 614.
[51] A. El Hamdaoui, G. Bergeret, J. Massardier, M. Primet, A. Renouprez, J. Catal. 148 (1994) 47.
[52] C. Descorme, P. Gélin, C. Lécuyer, M. Primet, J. Catal. 177 (1998) 352.
[53] A. Palazov, C.C. Chang, R.J. Kokes, J. Catal. 36 (1975) 338.
[54] Y.A. Lokhov, A. Davydov, Kinet. Katal. 21 (1980) 1515, 1523.
[55] D. Tessier, A. Rakai, F. Bozon-Verduraz, J. Chem. Soc., Faraday Trans. 88 (1992) 741.
[56] N. Sheppard, T.T. Nguyen, in: R.J.H. Clark, R.E. Hester (Eds.), Advances in IR and Raman Spectroscopy, Vol. 5, Wiley, New York, 1978, p. 67.
[57] R.L. Keiski, M. Hrkönen, A. Lahti, T. Maunula, A. Savimäki, T. Slotte, Catalysis and automotive pollution control III, Stud. Surf. Sci. Catal. 96 (1995) 85.
[58] K. Almusaiteer, S.S.C. Chuang, J. Catal. 180 (1998) 161.
[59] P.G. Harrison, E.W. Thornton, J. Chem. Soc., Faraday Trans. I 74 (1978) 2604.
[60] P.G. Harrison, E.W. Thornton, J. Chem. Soc., Faraday Trans. I 74 (1978) 2703.
[61] L. Genzel, T.P. Martin, Surf. Sci. 34 (1973) 33.
[62] M. Ocana, V. Fornès, J.V. Garcia Ramos, C.J. Serna, J. Solid State Chem. 75 (1988) 364.
[63] D. Amalric-Popescu, J.M. Herrmann, A. Ensuque, F. Bozon-Verduraz, Phys. Chem. Chem. Phys. 3 (2001) 2522.
[64] K. Almusaiteer, S.S.C. Chuang, J. Catal. 184 (1999) 189.